Draft version October 14, 2015
Preprint typeset using LaTeX style emulateapj v. 5/2/11

arXiv:1510.03821v1 [astro-ph.GA] 13 Oct 2015

TACKLING THE SATURATION OF OXYGEN: THE USE OF PHOSPHORUS AND SULPHUR AS PROXIES WITHIN THE NEUTRAL ISM OF STAR-FORMING GALAXIES

B. James[1,2] and A. Aloisi[2]
1. Institute of Astronomy, Madingley Road, Cambridge, CB3 0HA, UK and
2. Space Telescope Science Institute, Baltimore, MD 21218

Draft version October 14, 2015

ABSTRACT

The abundance of oxygen in galaxies is widely used in furthering our understanding of galaxy formation and evolution. Unfortunately, direct measurements of O/H in the neutral gas are extremely difficult to obtain due to the fact that the only O I line available within the HST UV wavelength range (1150–3200 Å) is often saturated. As such, proxies for oxygen are needed to indirectly derive an O/H via the assumption that solar ratios based on local Milky Way sight lines hold in different environments. In this paper, we assess the validity of using two such proxies, P II and S II, within more typical star-forming environments. Using HST-COS FUV spectra of a sample of nearby star-forming galaxies, we find that P and S follow a trend, $\log(\mathrm{P\,II/S\,II}) = -1.73 \pm 0.18$, which is in excellent agreement with the solar ratio of $\log(\mathrm{P/S})_\odot = -1.71 \pm 0.04$ over a large range of galaxy properties, i.e., metallicities in the range 0.03–3.2 $\mathrm{Z}_\odot$ and H I column densities of $\log[N(\mathrm{H\,I})/\mathrm{cm}^{-2}] = 18.44$–$21.28$. We additionally show evidence from literature data that both elements are individually found to trace oxygen according to their respective solar ratios across a wide-range of environments, such as stars, ionized gas in nearby galaxies, and neutral gas in DLAs and along Milky Way sight lines. Our findings demonstrate that the solar ratios of $\log(\mathrm{P/O})_\odot = -3.28 \pm 0.06$ and $\log(\mathrm{S/O})_\odot = -1.57 \pm 0.06$ can both be used to derive reliable O/H abundances in the neutral gas of local and high-redshift star-forming galaxies.

Subject headings: galaxies: ISM – galaxies: starburst – ISM: abundances – ultraviolet: ISM

1. INTRODUCTION

Oxygen is one of the most abundant elements in the Universe and is of prime importance in understanding the chemical evolution of galaxies. Its nucleosynthesis is well known and its abundance is therefore widely used to estimate the metallicity of different Galactic and extragalactic ISM gas phases. In particular, oxygen has been extensively investigated to derive H II region metallicities as it has several strong emission lines in the optical rest frame. However, constraining the oxygen content in the *neutral* gas of a galaxy through UV absorption line studies can be challenging. Within the UV wavelength range covered by HST (∼1150–3200 Å), at low redshift the most easily observed O I absorption lines are at 1302 Å and 1355 Å; the former is usually heavily saturated whilst the latter is usually too weak to be seen.

This challenging scenario often forces us to rely on a selection of elements that can, in principle, be used as proxies for oxygen. The most suited elements for this purpose are the ones that can trace oxygen, i.e., elements that (1) deplete onto dust in a similar way to oxygen, and (2) have the same nucleosynthetic origin as oxygen. The extent of an element's depletion onto dust grains is largely governed by the condensation temperature of that element. Oxygen (along with carbon and nitrogen) has a relatively low condensation temperature which prevents it from depleting easily onto dust grains. Conversely, refractory elements (e.g., silicon) can be largely depleted onto dust grains. Suitable oxygen-proxy candidates should therefore have a low condensation temperature and also be α elements, i.e., those that arise from the same α-capture production processes as oxygen.

The element traditionally used as a proxy to oxygen is sulphur (e.g., Pettini et al. 2002; Battisti et al. 2012; Berg et al. 2013b). Below 3200 Å, the singly ionized form of sulphur (S II) is detected through a triplet at 1250.6, 1253.8, and 1259.5 Å. Like oxygen, sulphur is an α element and both elements show the same dust depletion characteristics (Savage & Sembach 1996). In addition to this, ionization corrections for S II are found to be negligible when $\log[N(\mathrm{H\,I})/\mathrm{cm}^{-2}] \gtrsim 20.5$ and gas metallicities are sub-solar (James et al. 2014, J14 hereafter). S II can, however, suffer from saturation. In a recent study of 243 sight lines in the Milky Way (MW), Jenkins (2009) (J09 hereafter) found only 9 unsaturated S II lines.

There is one other suitable oxygen-proxy candidate at our disposal within the UV wavelength range: phosphorus. The dominant ionization stage of P in the neutral medium is P II. Several P II lines lie within the HST UV wavelength range, the strongest being at 1152 Å and 1301 Å. However, unlike oxygen and sulphur, phosphorus is believed to be a neutron-capture element, probably formed in the carbon and neon burning shells during the late stages of the evolution of massive stars (Arnett 1996), and its relatively high condensation temperature suggests that it should be more heavily depleted. Despite this, in studies of the ISM towards stars within the MW it has been shown that P II is not depleted along sight lines containing predominantly warm low-density neutral gas (Jenkins 1986) or diffuse neutral gas (Lebouteiller et al. 2005, L05 hereafter). Using ten unsaturated P II measurements towards local stars combined with several Galactic and extragalactic sight lines (all with $\log[N(\mathrm{H\,I})/\mathrm{cm}^{-2}] \geq 20.94$), L05 found that P II and O I column densities relate to each other in solar P/O proportions (i.e., no differential depletion of P II and O I),

suggesting that phosphorus could be a suitable tracer of oxygen in extragalactic regions. Contrary to this, J09 found that phosphorus depletes onto dust grains more rapidly than oxygen in the MW, a more metal-rich environment. With regards to stellar abundances, there have been very few measurements for phosphorus, namely because P II lines are absent in the ordinary wavelength range of stellar spectra. However, in a recent study using high-resolution infrared spectroscopy of cool stars in the Galactic disk, Caffau et al. (2011) found that the ratio between phosphorus and sulphur is roughly constant with metallicity and consistent with the solar value.

Since the majority of data concerning the relative depletions of S and P with respect to O, arises from sight lines within the local ISM, it is unclear whether these relationships only hold within similar environments, i.e., intermediate–solar metallicities[1] and relatively high column densities ($\log[N(\mathrm{H\,I})/\mathrm{cm}^{-2}] \gtrsim 20$). This of course presents a serious problem as we enter an era where the improved sensitivity of instruments enables increasing access to the high-resolution rest-frame UV spectra of high-z galaxies, and the need to invoke proxies for oxygen in environments that are rather different to the Milky Way becomes more frequent. Moreover, if we were to compare chemical abundances across different gas *phases*, we would most benefit by constraining O/H from the neutral gas absorption line profiles because of the common use of oxygen as metallicity indicator within the nearby universe. As of now, when comparing metallicities across cosmic time, high-z observations are often forced to rely on elements that have a different nucleosynthetic origin to oxygen (e.g., Fe/H, Lilly et al. 2003). In this letter we aim to offer a solution to the problem of assessing oxygen abundances in the neutral gas by demonstrating the reliability of sulphur and phosphorus as proxies for oxygen across a range of galaxy environments.

2. DATA ANALYSIS (AN OVERVIEW)

The data utilized within this paper originate from a series of publications regarding an investigation of nearby star-forming galaxies (SFGs) using *HST*-COS (PID: 11579, PI: Aloisi). The project involved 26 orbits of COS spectroscopy with the G130M grism at λ_c=1291 Å. The sample of SFGs contains a range of galaxy types (i.e., blue compact dwarfs, mergers, and spirals), with oxygen metallicities of $\sim$0.03–3.2 $\mathrm{Z}_\odot$ and distances of $\sim$3–54 Mpc. Full details of the targets, observations, data reduction, and analysis techniques can be found in J14.

Table 1 lists the column densities of H I, O I, P II, and S II measured within each galaxy's spectrum. H I column densities were measured from the Lyα profile and are in the range $\log[N(\mathrm{H\,I})/\mathrm{cm}^{-2}] \sim 18.4$–$21.7$. Overall, column densities for O I and P II were measured using O I λ1302 and P II λ1152, while for S II the triplet $\lambda\lambda\lambda$1250, 1253 and 1259 was used. A description of the specific lines used for each galaxy and pointing can be found in J14, along with their corresponding line profiles and a full description of the assessment of saturation.

Ad-hoc photoionization models specific to the metallicity and H I column density of each galaxy were used by J14 to estimate ionization correction factors (ICFs) to account for both classical ionization and contamination of ionized gas along the line of sight. For O I, S II, and P II, ICFs were found to be negligible for almost all galaxies, i.e., each of these ions was found to be the dominant ionization stage of the species within the neutral gas and was found not to be present within the ionized gas. The two exceptions are M83-Pos.1 and NGC 3690_{v2}, where ICF corrections are $\sim$0.15–0.24 dex for both P II and S II, and $\sim$0.01–0.03 dex for O I, mostly due to their high metallicities and the relatively low H I column densities. All column densities listed in Table 1 and used hereafter have been corrected for ionization using the total ICF values listed in J14 (their Table 8). Model ICF values were unobtainable for M83-Pos.2 due to its exceptionally low H I column density, and we therefore use only upper limit column densities throughout.

TABLE 1
Logarithmic Column Densities of H I, O I, P II, & S II within the Sample

Galaxy	$\log[N(\mathrm{H\,I})]$	$\log[N(\mathrm{O\,I})]$	$\log[N(\mathrm{P\,II})]$	$\log[N(\mathrm{S\,II})]$
I Zw 18	21.28 ± 0.03	> 14.80	...	14.72 ± 0.05
SBS 0335−052	21.70 ± 0.05	> 14.77	12.96 ± 0.15	14.96 ± 0.03
SBS 1415+437	21.09 ± 0.03	> 14.87	13.41 ± 0.08	14.94 ± 0.03
NGC 4214	21.12 ± 0.03	> 15.25	13.74 ± 0.04	15.55 ± 0.03
NGC 5253-Pos.1	21.20 ± 0.01	> 15.44	13.73 ± 0.08	15.43 ± 0.02
NGC 5253-Pos.2	20.65 ± 0.05	> 15.31	13.60 ± 0.12	15.33 ± 0.04
NGC 4670	21.07 ± 0.08	> 15.26	13.80 ± 0.05	> 15.58
NGC 4449	21.14 ± 0.03	> 15.54	14.09 ± 0.09	15.60 ± 0.09
NGC 3690_{v1}	20.62 ± 0.02	> 15.48	...	15.39 ± 0.05
NGC 3690_{v2}	19.81 ± 0.08	> 14.84	...	...
M83-Pos.1	19.59 ± 0.32	...	13.84 ± 0.26	15.39 ± 0.25
M83-Pos.2	< 18.44	...	< 13.73	< 15.39

Notes: All column densities refer to ICF-corrected values.

3. RESULTS

3.1. *Column density trends with metallicity*

Figure 1 shows column densities of H I, S II, and P II against metallicity (Table 2). These plots illustrate the wide range in metallicity and H I column density covered by our sample, and show that clear relationships exist between the metallicity and column density of each species.

Firstly, the anti-correlation between metallicity and $N(\mathrm{H\,I})$ is clearly apparent: the object with the lowest H I column density (M83) lies at $\sim$ 3 $\mathrm{Z}_\odot$ and the objects with the highest H I column density (I Zw 18 and SBS 0335−052) lie well below $\mathrm{Z}_\odot$. This is possibly due to the dilution of chemically enriched gas in the less massive and more metal-poor SFGs, e.g., by accretion of more primordial gas. Secondly and perhaps unsurprisingly, as the metallicity of the ionized gas increases, so do the column densities of the S II and P II ions.

3.2. *A solar relationship?*

As discussed previously, the use of certain elements as tracers for oxygen stems from the relationships observed between those elements and oxygen mostly within the Galactic neighborhood. In order to directly see one of these relationships, in the left panel of Fig. 2 we plot the column densities of P II as a function of O I using values from J09[2] (measured from 243 sight lines within the

[1] We define metallicity as 12+log(O/H), where O/H refers to the oxygen abundance of the ionized gas. In this scale the solar metallicity corresponds to 12+log(O/H) = 8.69 ± 0.05 (Asplund et al. 2009, A09 hereafter).

[2] Whilst the lines used for N(P II) and N(S II) are not explicitly listed by J09, strict censorship rules were employed to ensure that saturated lines were not included within the sample.

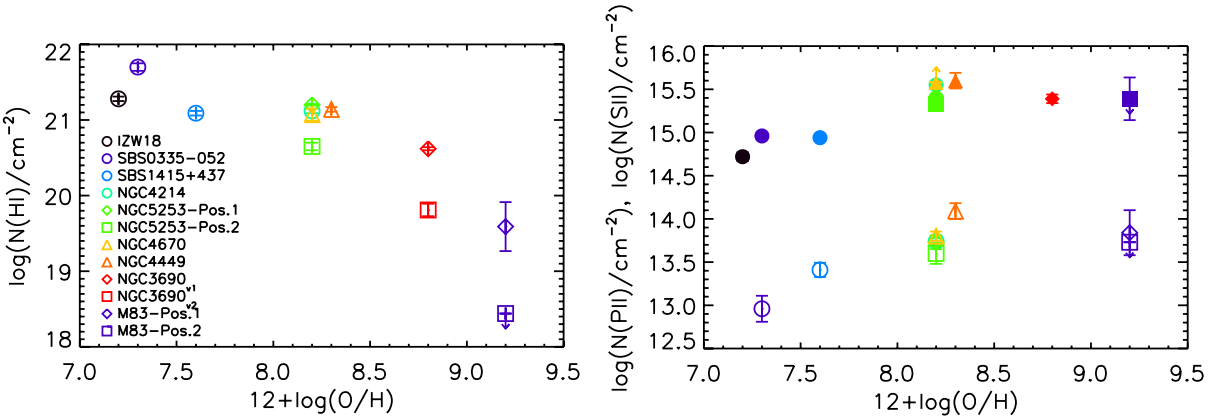

FIG. 1.— *Left panel:* metallicity vs. N(H I); *right-panel:* metallicity vs. N(P II) and N(S II) (open and filled symbols). In the case of I Zw 18, the P II λ1152 absorption line was not detected in the spectrum, so N(P II) is not available. Column densities are listed in Table 1.

MW) and from L05 (towards Galactic stars measured within their study or compiled from the literature).

Also shown in the same panel are the O I and P II column densities measured for local ($0.083 < z_{abs} < 0.321$) DLAs from Battisti et al. (2012)[3], and high-z DLAs from Dessauges-Zavadsky et al. (2004, 2006). Despite the fact that our literature O and P data compilation covers different environments, ranging from the local solar-metallicity neighborhood of MW sight lines, to metal-poor high-z DLA systems, it can be seen that all points lie roughly along the solar P/O ratio[4]. From these literature data, and excluding those values that are limits, we find the error-weighted mean ratio of $\log(\text{P II/O I}) = -3.30 \pm 0.24$ (blue solid line with the $\pm 1\sigma$ errors indicated as blue dashed lines), which is in good agreement with the solar ratio of $\log(\text{P/O})_\odot = -3.28 \pm 0.06$ (green solid and dashed lines). Data from our sample (J14) are also plotted in the left panel of Fig. 2 (red solid circles). However, due to the lower limits of the O I column densities, it was not possible to calculate a mean ratio from this sample.

We also determined whether P II and S II follow a solar ratio within local SFGs. As discussed previously, sulphur exists as a triplet of lines with relatively weak oscillator strengths and has almost zero affinity to dust. Indeed, in our sample (J14) only one galaxy (NGC 4670) harbored S II lines that were affected by saturation. The middle panel of Fig. 2 shows the column density of P II versus that of S II within our sample (red solid circles) along with the error-weighted mean column density ratio of $\log(\text{P II/S II}) = -1.73 \pm 0.18$ (red solid and dashed lines), which is in good agreement with the solar ratio of $\log(\text{P/S})_\odot = -1.71 \pm 0.04$.

Also included in the middle panel of Fig. 2 are the S II and P II column densities of the local and extra-galactic ISM by L05 as well as a couple of MW sight lines from J09 (due to the high-column densities involved, S II was saturated in most targets of this sample), along with high-redshift (Dessauges-Zavadsky et al. 2004, 2006) and low-redshift (Battisti et al. 2012) DLAs. When we include all (non-limit) measurements from the literature, we find a mean ratio of $\log(\text{P II/S II}) = -1.80 \pm 0.26$, which is again in agreement with the solar ratio[5]. This result is in agreement with Caffau et al. (2011), where the [P/S] ratio was found to be roughly constant within 0.1 dex in 20 cool stars of the Galactic disk (see their Fig. 4), implying that P and S are produced in the same amounts over the $-1.0 < [\text{Fe/H}] < +0.3$ metallicity range considered.

Unfortunately, due to saturation issues affecting both S and O, the plot of N(S II) versus N(O I) for MW sight lines, ISM of local SFGs, and DLAs, is rather unavailing (right panel of Fig. 2). However, we can assess the relationship between S and O in stars with $T \sim 5000$–6500 K (Nissen et al. 2007; Berg et al. 2013b), and ionized gas within local metal-poor SFGs (Izotov et al. 2006; López-Sánchez & Esteban 2010) and spiral galaxies (e.g., Berg et al. 2013a). This relationship is found to be solar in each of these studies ($\log(S/O)_\odot = -1.57 \pm 0.06$). This is of course as expected since both S and O are α-capture elements and therefore evolve in parallel in the ISM from the time they are produced in stars until they are ejected and well mixed into the ISM.

To summarize, P II and S II follow a solar ratio in our sample of nearby SFGs, similarly to what happens for a compilation of literature data representing a variety of environments. This is somewhat expected, since sulphur and phosphorus are both products of massive stars, even though they have different nucleosynthetic origins. If we combine this result with the fact that P II and O I follow a solar ratio in the same literature sample, we can conclude that both P II and S II can indeed be used as proxies for oxygen in a variety of environments, including in the neutral gas of our nearby SFGs.

4. DISCUSSION AND CONCLUSIONS

Based on the above findings, we can now obtain O abundances for our sample of SFGs by using P and S column densities and applying the P/O and

[3] For each comparison sample, column densities resulting from saturated profiles are shown as lower limits. For the Battisti et al. (2012) sample, upper limits refer to undetected lines and were derived from a 3σ upper limit on the equivalent width, assuming the line is on the linear part of the curve of growth.

[4] J09 found that in fact phosphorus depletes onto dust grains more rapidly than oxygen, as demonstrated in their paper by an oxygen depletion slope that is considerably less than that of phosphorus. However, the left panel of Fig. 2 shows that P and O are still in a solar ratio in the MW sight lines probed by J09.

[5] For reference, J09 found the slope of sulphur depletion to be in agreement with that of phosphorus within the uncertainties.

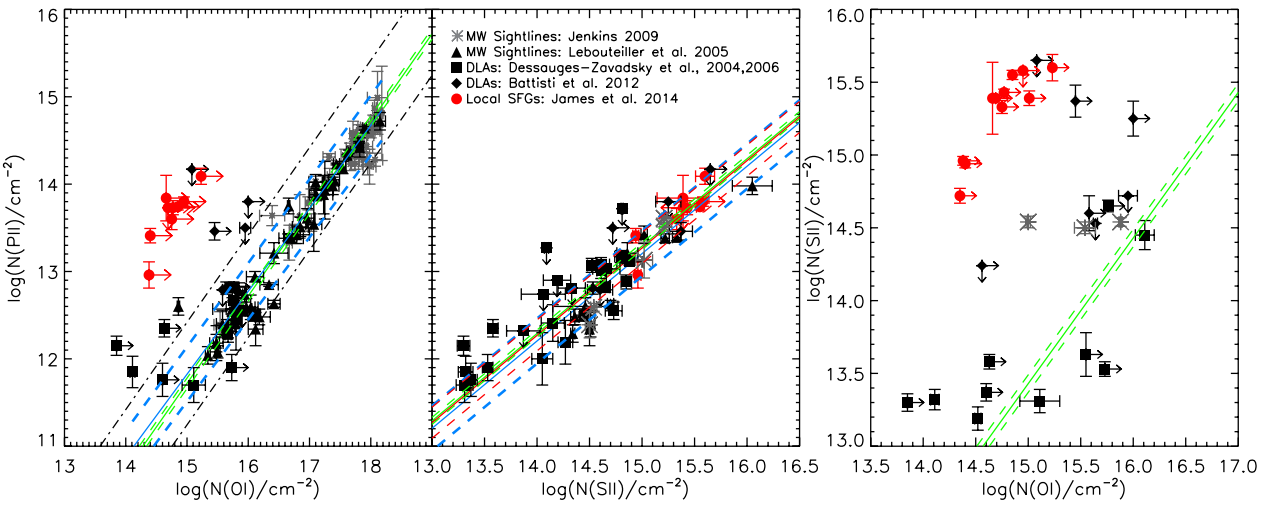

FIG. 2.— Relationship between P II, O I, and S II column densities within local SFGs (red dots; J14). Also shown (black symbols) are those measured from MW sight lines (Jenkins 2009; Lebouteiller et al. 2005) and DLAs (Dessauges-Zavadsky et al. 2004, 2006; Battisti et al. 2012). *Left panel:* blue line represents weighted mean ratio between the compilation of O I and P II column densities (excluding limits) of log(P II/O I) = −3.30 ± 0.24; green line represents solar ratio of $\log(P/O)_\odot = -3.28 \pm 0.06$ (A09); black dot-dash lines represent upper and lower limits of log(P/O) derived from maximum and minimum depletions along the sight line in J09. *Middle panel:* red line corresponds to weighted mean ratio of log(P II/S II) = −1.73 ± 0.18 measured from the J14 sample; blue line represents weighted mean ratio of log(P II/S II) = −1.80 ± 0.26 from literature values; green line represents solar ratio of $\log(P/S)_\odot = -1.71 \pm 0.04$ (A09). *Right panel:* green line represents solar ratio of $\log(S/O)_\odot = -1.57 \pm 0.06$ (A09). In each case, dashed lines represent the $\pm 1\sigma$ values.

TABLE 2
OXYGEN ABUNDANCES DERIVED FROM PHOSPHORUS AND SULPHUR COLUMN DENSITIES

Galaxy	log(O_P/H)	log(O_S/H)	⟨log(O/H)⟩	[O/H]$_{HI}$	12+log(O/H)$_{HII}$	[O/H]$_{HII}$
I Zw 18	...	−4.99 ± 0.08	−4.99 ± 0.08	−1.68 ± 0.09	7.2	−1.49
SBS 0335−052	−5.46 ± 0.17	−5.17 ± 0.08	−5.22 ± 0.07	−1.92 ± 0.09	7.3	−1.39
SBS 1415+437	−4.40 ± 0.10	−4.58 ± 0.07	−4.52 ± 0.06	−1.21 ± 0.08	7.6	−1.09
NGC 4214	−4.10 ± 0.08	−4.00 ± 0.07	−4.04 ± 0.05	−0.74 ± 0.07	8.2	−0.49
NGC 5253-Pos.1	−4.19 ± 0.10	−4.20 ± 0.06	−4.20 ± 0.05	−0.89 ± 0.07	8.2	−0.49
NGC 5253-Pos.2	−3.77 ± 0.14	−3.75 ± 0.09	−3.76 ± 0.08	−0.45 ± 0.09	8.2	−0.49
NGC 4670	−3.99 ± 0.11	> −3.92	−3.99 ± 0.11	−0.68 ± 0.12	8.2	−0.49
NGC 4449	−3.77 ± 0.11	−3.97 ± 0.11	−3.87 ± 0.08	−0.56 ± 0.09	8.3	−0.39
NGC 3690$_{v1}$	...	−3.66 ± 0.08	−3.66 ± 0.08	−0.35 ± 0.09	8.8	+0.11
NGC 3690$_{v2}$	...	...	...	...	8.8	+0.11
M83-Pos.1	−2.47 ± 0.42	−2.63 ± 0.41	−2.55 ± 0.29	+0.76 ± 0.29	9.2	+0.51
M83-Pos.2	< −1.43	< −1.48	< −1.46	< +1.86	9.2	+0.51

Notes: [O/H] = log(O/H) − log(O/H)$_\odot$. Average oxygen abundance [O/H]$_{HI}$ refers to weighted mean ⟨log(O/H)⟩, except for cases where only one non-limited value exists. 12+log(O/H)$_{HII}$ and [O/H]$_{HII}$ values refer to ionized gas metallicities (see Table 1 in J14).

S/O solar ratios. In Table 2 we list O_P/H and O_S/H which represent O/H calculated by using P and S as proxy, respectively. We also list the mean O abundance derived from both values, ⟨log(O/H)⟩, and its value with respect to the solar abundance, [O/H]$_{HI}$. For comparison, we also list [O/H]$_{HII}$, the ionized gas abundances from the values 12+log(O/H)$_{HII}$ measured from emission-line spectroscopy. Excluding limits, the mean difference between ionized and neutral gas abundances is $\langle [O/H]_{HII} - [O/H]_{HI} \rangle = 0.20 \pm 0.23$. This means that by adopting the proxies here described for the neutral gas of our SFGs we can recover the O abundances of their ionized gas within a factor of 2. The agreement between the abundances of the two gas phases can be clearly seen in Fig. 3, where we plot [O/H]$_{HII}$ versus [O/H]$_{HI}$. The similarity of the O abundance in the neutral and ionized gas of our sampled SFGs should not be taken for granted, but rather as indication that the gas is well mixed. For an in-depth discussion of this issue, we refer the reader to Paper II of our COS analysis series (Aloisi et al., in prep).

As we have now established that both S and P are reliable tracers of O in the neutral ISM, a question remains as to whether circumstances exist where one proxy is more suitable than the other. This can be evaluated via the properties of each species. Firstly, their affinity to become saturated can be assessed using the curve of growth (COG), which plots log $(N \times f \times \lambda)$ against log (W/λ) (where N = column density, f = oscillator strength, λ = wavelength, and W = equivalent width) - i.e., the location of an absorption line along the COG can reveal whether or not the line is saturated (see, e.g., J14). Both P II λ1152 and the weakest of the S II triplet, S II λ1250, fall on the same part of the COG. Using the column densities of Table 1, for P II λ1152 and S II λ1250 (with $f = 2.361 \times 10^{-1}$ and $f = 5.453 \times 10^{-3}$, respectively; see Morton 1991), we obtain averages of $\log(Nf\lambda) = 8.171$ and 8.174, respectively. As they lie so close on the COG, there would be few circumstances when one would

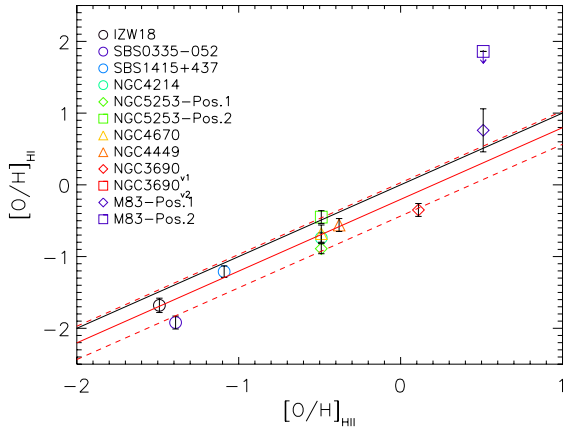

FIG. 3.— Comparison between proxy-derived oxygen abundances in the neutral gas, $[O/H]_{HI}$, and ionized gas abundances, $[O/H]_{HII}$. Excluding limits, we find $\langle[O/H]_{HII}-[O/H]_{HI}\rangle = 0.20 \pm 0.23$ (represented by red solid and dashed lines). Black solid line represents 1:1 ratio.

become saturated without the other. It should be noted that while P II λ1301 lies slightly lower on the COG ($f = 1.271\times10^{-2}$, giving $\log(Nf\lambda) = 6.957$ on average), the line is heavily contaminated with O I λ1302 and therefore unusable. The third P II line within the HST-UV wavelength range, P II λ1532, is $\sim$30 times fainter than P II λ1301 and therefore not easily detected. If only one or both of the other S II triplet lines are available instead of S II λ1250, then there will be cases where S II is saturated and P II is not; e.g., this is the case for NGC 4670 in all the sight lines studies within J14.

With regards to their wavelength, having only $\sim$100 Å separation between P II λ1152 and S II λ1250 means that they are both readily accessible within the FUV spectrum and cases where only S II or P II is available would be most likely rare (unless one of the two is blended, e.g., with a MW absorption). On the other hand, this does mean that the observer will benefit from two oxygen-proxy elements within a single spectrum, thereby providing a more accurate oxygen abundance determination.

A small difference does exist between the ionization potentials of P II (19.76946 eV) and S II (23.33788 eV) (Morton 2003). As such, environments may exist where the strength of the ionizing source may affect one species more than another, e.g., along sight lines that have low H I column density. In such cases, P II would be more easily ionized than S II and a larger portion of P would exist as P III in the ionized gas. This could of course be corrected for by applying adequate ICFs (as seen in Table 8 of J14).

Overall it can be seen that *both* P II and S II can provide a mean for deriving accurate oxygen abundances in the neutral ISM of SFGs. Using our sample of local SFGs (J14), we have shown that P/S follows the solar ratio of $\log(P/S)_\odot = -1.71\pm0.04$ across a wide range of H I column densities ($\log[N(H\,I)/cm^{-2}] = 18.44$–$21.28$) and metallicities (0.03–3.2 $Z_\odot$), with an average of $\log(P\ II/S\ II) = -1.73 \pm 0.18$. We have additionally demonstrated from the literature that ratios of $\log(P\ II/S\ II) = -1.80 \pm 0.26$ and $\log(P\ II/O\ I) = -3.30 \pm 0.24$ for sight lines throughout a wide range of environments, such as DLAs (similar to our sample of SFGs) and the MW, are also in very good agreement with solar values ($\log(P/O)_\odot = -3.28 \pm 0.06$). By combining these two pieces of information with the fact that S/O also follows the solar ratio of $\log(S/O)_\odot = -1.57 \pm 0.06$ in stellar abundances and the ionized gas within SFGs, we suggest that both P and S can reliably trace O throughout the neutral gas of typical SFGs.

By covering a large range in ISM properties, and in particular extending down to significantly low-metallicity, we can ensure that the application of a P/O and S/O solar ratio to infer O from P and S can be both numerous and widespread. In particular, the derivation of neutral ISM oxygen abundances in high-z systems can now be derived with a higher level of certainty, either from using P or S, or by using the solar relationships to check whether the measured O/H is based on a unsaturated line or not. We hope the relations derived within this work will aid future studies in comparing oxygen abundances across different gas phases and enable oxygen abundance measurements throughout cosmic time.

REFERENCES

Arnett D., 1996, Supernovae and Nucleosynthesis: An Investigation of the History of Matter from the Big Bang to the Present

Asplund M., Grevesse N., Sauval A. J., Scott P., 2009, ARA&A, 47, 481

Battisti A. J., Meiring J. D., Tripp T. M., Prochaska J. X., Werk J. K., Jenkins E. B., Lehner N., Tumlinson J., Thom C., 2012, ApJ, 744, 93

Berg D. A., Skillman E. D., Garnett D. R., Croxall K. V., Marble A. R., Smith J. D., Gordon K., Kennicutt Jr. R. C., 2013a, ApJ, 775, 128

Berg T. A. M., Ellison S. L., Venn K. A., Prochaska J. X., 2013b, MNRAS, 434, 2892

Caffau E., Bonifacio P., Faraggiana R., Steffen M., 2011, A&A, 532, A98

Dessauges-Zavadsky M., Calura F., Prochaska J. X., D'Odorico S., Matteucci F., 2004, A&A, 416, 79

Dessauges-Zavadsky M., Prochaska J. X., D'Odorico S., Calura F., Matteucci F., 2006, A&A, 445, 93

Izotov Y. I., Stasińska G., Meynet G., Guseva N. G., Thuan T. X., 2006, A&A, 448, 955

James B. L., Aloisi A., Heckman T., Sohn S. T., Wolfe M. A., 2014, ApJ, 795, 109

Jenkins E. B., 1986, ApJ, 304, 739

—, 2009, ApJ, 700, 1299

Lebouteiller V., Kuassivi, Ferlet R., 2005, A&A, 443, 509

Lilly S. J., Carollo C. M., Stockton A. N., 2003, ApJ, 597, 730

López-Sánchez Á. R., Esteban C., 2010, A&A, 517, A85

Morton D. C., 1991, ApJS, 77, 119

—, 2003, ApJS, 149, 205

Nissen P. E., Akerman C., Asplund M., Fabbian D., Kerber F., Kaufl H. U., Pettini M., 2007, A&A, 469, 319

Pettini M., Ellison S. L., Bergeron J., Petitjean P., 2002, A&A, 391, 21

Savage B. D., Sembach K. R., 1996, ApJ, 470, 893

We gratefully acknowledge Max Pettini for useful discussions and insightful comments on this manuscript. STScI is operated by the Association of Universities for Research in Astronomy, Inc., under NASA contract NAS5-26555.